Research Article

Received: 10 December 2023 Revised: 7 February 2024 Accepted article published: 10 February 2024 Published online in Wiley Online Library: 25 February 2024

(wileyonlinelibrary.com) DOI 10.1002/jctb.7620

Enhancing bioelectricity generation from wastewater in microbial fuel cells using carbon nanomaterials

Yasser A Attia,[a*] Mohamed Samer,[b] Mahmoud SM Mohamed,[c] Mohamed Salah,[a] Elshaimaa Moustafa,[b] R M Abdel Hameed,[d] Hassan Elsayed[e] and Essam M Abdelsalam[a]

Abstract

BACKGROUND: Microbial fuel cells (MFCs) offer a promising approach for treating wastewater and generating electrical energy simultaneously. However, their implementation in wastewater treatment plants is hindered by the limited electricity generation, often attributed to the electrolyte's high resistance. This study aimed to improve bioelectricity generation in MFCs by adding nanomaterials to the electrolyte to enhance conductivity.

RESULTS: Three types of nanomaterials – carbon nanotubes (CNTs), graphitic carbon nitride (g-C_3N_4), and reduced graphene oxide (r-GO) – were synthesized and addition to the electrolyte at a concentration of 50 mg in 1.5 L. MFC performance was evaluated, employed a hydraulic retention time (HRT) of 140 h, and compared to a control with no nanomaterials added. The addition of nanomaterials significantly improved MFC performance. Compared to the control, the MFCs with CNTs, g-C_3N_4, and r-GO exhibited higher voltage: 1.301 V (CNTs), 1.286 V (g-C_3N_4), 1.280 V (r-GO) *versus* 0.570 V (control); increased power density: 14.11 mW m^{-3} (CNTs), 13.78 mW m^{-3} (g-C_3N_4), 13.66 mW m^{-3} (r-GO) *versus* 2.71 mW m^{-3} (control); enhanced areal power density: 21.06 mW m^{-2} (CNTs), 20.57 mW m^{-2} (g-C_3N_4), 20.39 mW m^{-2} (r-GO) *versus* 4.04 mW m^{-2} (control); and improved coulombic efficiency: 19.43% (CNTs), 19.19% (g-C_3N_4), 19.11% (r-GO) *versus* 8.54% (control).

CONCLUSION: Incorporating nanomaterials into the MFC electrolyte significantly increased bioelectricity generation by 5.21 times and coulombic efficiency by 2.28 times compared to the control. This improvement is attributed to the high specific surface area of the nanomaterials, which facilitates the adhesion and growth of microorganisms around the anode, enhancing direct electron transfer.

Keywords: microbial fuel cells; nanotechnology; microorganism; bioelectricity generation; wastewater treatment; electrolyte conductivity

INTRODUCTION

Microbial fuel cells (MFCs) are bioelectrochemical appliances consisting of electroactive microorganisms that generate electrons while oxidizing organic materials.[1] Not only do MFCs treat wastewater, but they also convert organic matter in the wastewater into usable energy. Consequently, MFCs represent a new and promising approach for generating power, where wastewater treatment plants can be upgraded to power plants. Bacteria use the anode as bedding where they oxidize organic materials and release electrons under anaerobic conditions inside the anode chamber. However, the introduction of air to the cathode chamber facilitates the reduction of dissolved oxygen (O_2) at the cathode, promoting the flow of electrons from the anode through the external circuit to the cathode, resulting in the production of electrical energy.[2-5] Compared to other methods of producing energy from organic materials, MFCs have benefits. First, significant conversion efficiencies are possible with direct substrate to electrical conversion. Second, they do not need to process the methane the cell produces. Third, they do not require additional energy to aerate the cathode, given that it can be aerated passively. Fourth, they offer a further renewable energy option to address the world's energy needs because they may be used in rural locations lacking electrical infrastructure. Furthermore, because MFCs use

* Correspondence to: YA Attia, National Institute of Laser Enhanced Sciences (NILES), Cairo University, 12613 Giza, Egypt. E-mail: yasserniles@niles.cu.edu.eg

a National Institute of Laser Enhanced Sciences (NILES), Cairo University, Giza, Egypt

b Department of Agricultural Engineering, Faculty of Agriculture, Cairo University, Giza, Egypt

c Department of Botany and Microbiology, Faculty of Science, Cairo University, Giza, Egypt

d Department of Chemistry, Faculty of Science, Cairo University, Giza, Egypt

e Department of Microbial Biotechnology, Biotechnology Research Institute, National Research Centre, Giza, Egypt

an anaerobic process, the amount of bacterial biomass produced will be lower than in an aerobic system.[6-9] More than 30 pure isolates were reported in MFC studies, and the mainstream exoelectrogens include *Geobacter*, *Shewanella*, and *Pseudomonas*. Additionally, some other exoelectrogens were recognized – for instance, *Acidiphilium* sp., *Arcobacter butzleri*, *Aeromonas hydrophila*, *Aeromonas* sp., *Bacillus subtilis*, *Clostridium butyricum*, *Desulfuromonas acetoxidans*, *Desulfobulbus propionicus*, *Desulfovibrio desulfuricans*, *Escherichia coli*, *Enterobacter cloacae*, *Geothrix fermentans*, *Geopsychrobacter electrodiphilus*, *Klebsiella pneumonia*, *Ochrobactrum anthropi*, *Pichia anomala*, *Rhodoferax ferrireducens*, *Rhodopseudomonas palustris*, *Thermincola* sp., and *Tolumonas osonensis*.[10] There is a range of designs of MFCs, where the conventional ones are single-chamber MFCs, double-chamber MFCs and stacked MFCs.[11,12] The maximum working temperature of standard MFCs is less than 80 °C, where the working temperature ranges from 25 to 70 °C.[13] Most studies operated the MFCs within a temperature range from 25 to 30 °C.[14,15] Another important factor is the pH, where the highest power densities occur at a pH of 6.7.[2] On the other hand, the hydraulic retention time (HRT) ranges from 14 to 20 days in most studies.[1,16] However, in practice, MFCs can be operated continuously for up to 150 days.[17]

Nanotechnology is a rapidly developing field that deals with the manipulation of matter at the atomic and molecular level. This means working with materials and structures that are between 1 and 100 nm in size – a nanometer being one billionth of a meter. At this scale, the properties of materials can change dramatically compared to their bulk counterparts. The possibilities are endless. Researchers are using nanotechnology to develop a wide range of new products and technologies, including (1) electronics: nanomaterials are being used to create smaller, faster and more efficient electronic devices; for example, quantum dots are being used to develop new types of displays and LEDs, while carbon nanotubes are being investigated for use in transistors and other components; (2) medicine: nanoparticles are being used to deliver drugs directly to diseased cells, which can improve the effectiveness of treatment and reduce side effects; they are also being used to develop new diagnostics and imaging techniques; (3) energy: nanomaterials are being used to develop more efficient solar cells, batteries, and fuel cells; they are also being investigated for use in carbon capture and storage technologies; and (4) environmental remediation: nanomaterials are being used to clean up contaminated soil and water. They are also being used to develop new techniques for recycling and waste management.[18-21] It is important to carefully consider both the potential benefits and risks of nanotechnology before developing and using this powerful technology.

Unfortunately, MFC's implementation in wastewater treatment plants is still restricted owing to some complications. Electrolyte resistance is estimated as the main issue hindering electricity production by MFCs.[12] Biofilm developed on the electrode surface plays a key role in MFC operation.[16,22] On the other hand, Rabaey and Verstraete[23] reported that losses in MFCs are due to (1) bacterial electron transfer; (2) electrolyte resistance; (3) anode resistance; (4) membrane resistance; (5) cathode resistance; and (6) electron acceptor reduction. Therefore, future research work should focus on implementing novel technologies to reduce these losses. Incorporating nanomaterials and nanocomposites into electrolytes holds promise for enhancing their conductivity, potentially leading to improvements in their conductivity. Consequently, the efficiency of the MFC increases. Additionally, nanomaterials are hypothesized to enhance the biofilm development process on the electrode surface. Conventional carbon materials have a 2D structure, which limits the area for driving power output due to an inefficient electronic transmission channel and a relatively high internal resistance.[7] The interface between the anode and the exoelectrogens is typically decorated using carbon-based nanomaterials.

MFCs are a fascinating technology that holds immense potential for sustainable wastewater treatment and bioenergy generation. However, their limitations in terms of power generation have hampered their widespread adoption. This is where nanotechnology emerges as a game changer, offering innovative solutions to enhance MFC performance and unlock its full potential. One of the key limitations in MFCs is the low conductivity of the electrolyte, which hinders electron transfer between microbes and electrodes. By incorporating conductive nanomaterials like carbon nanotubes (CNTs), graphene oxide (GO) and reduced graphene oxide (rGO) into the electrolyte, researchers can significantly improve conductivity, thereby promoting efficient electron transfer and boosting power generation.

The major goal of this research is to increase the efficiency of MFCs by using conductive carbon nanomaterials (CNTs, r-GO, and g-C_3N_4) as electrolyte additions. The following goals can be used to further this goal: following the addition of nanomaterials to the electrolyte, the efficiency of MFCs will be assessed, and the engineering parameters of coulombic efficiency, electrical current, voltage, resistance, power, power density, and areal power density will be examined.

MATERIALS AND METHODS

Manufacturing and installing the MFCs

MFCs were made of acrylic – that is, plexiglass (ACME Plastic, Miami USA). Each MFC has an elevation of 15 cm and 10 × 10 cm for the section. The system consists of two chambers (cathode and anode chambers), a salt bridge and a voltage/current measurement system (NI 9207 Spring, 16-channel), where the anode chamber was filled with a substrate volume of 1.5 L, and the cathode chamber was filled with a water volume of 1.5 L, as shown in Fig. 1.

Nanomaterial preparation

Preparation of r-GO

Graphene oxide (GO) was synthesized by implementing Hummer's technique.[24,25] To obtain r-GO from GO, 100 mg of the dry GO powder was put into a beaker that was covered with aluminum foil having punched pores and placed in a hood on a hot plate at 350 °C for 10 min. The resulting black powder of r-GO was collected.[26]

Preparation of carbon nanotubes (CNTs)

CNTs were fabricated by employing catalyst-free chemical vapor deposition (CVD) synthesis in nanoporous anodic alumina membranes (NAAMs). The synthesizing process was conducted by implementing a CVD structure comprising a two-stage furnace outfitted with a quartz tube, with a diameter of 43 mm and a length of 1000 mm, as well as temperature and gas flow controllers.[27,28]

Preparation of graphitic carbon nitride (g-C_3N_4)

g-C_3N_4 nanomaterials were prepared by heating 50 g urea at 550 °C in the air for 4 h.[26]

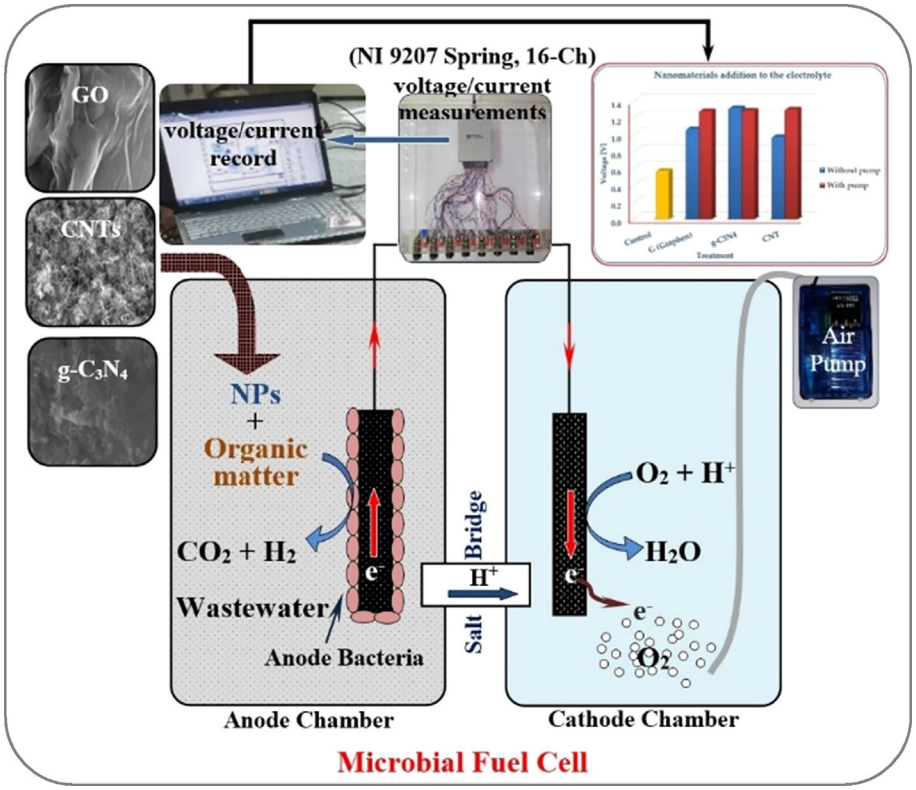

Figure 1. Graphical outline of MFC components, a voltage/current measurement and recording system with different carbon nanoadditives.

Nanomaterial characterization

Ultraviolet (UV)–visible spectra were quantified using a PerkinElmer Lambda 40 UV–visible spectrophotometer with 1 cm path length Hellma quartz cuvettes. Scanning electron microscopy (SEM) images were taken using a Zeiss FE-SEM ULTRA Plus (outfitted with EDX analyzer) microscope and Philips CM20 microscope, working at a voltage of 200 kV. Several drops from the specimen dispersion were placed onto an aluminum pin stub and left to evaporate at room temperature. X-ray diffraction (XRD) measurements were conducted by employing a Philips PW1710 X-ray diffractometer with Cu Ka radiation (k = 1.54186 A°). The XRD patterns were logged from 20° to 70° 2θ with a step size of 0.020° 2θ and gathering 10 s per step. Fourier transform infrared (FTIR) spectra were logged with a Nicolet 6700 infrared spectrophotometer to determine the specific functional groups available on the surface. Based on the Brunauer–Emmett–Teller (BET) model, the precise surface area and pore volume were calculated using a Micromeritics ASAP 2010 to collect N_2 sorption isotherms. The samples were first outgassed under vacuum at 60 °C overnight, before being examined at 77 K.

Waste handling

A sample of wastewater and sludge was collected from Zenein Wastewater Treatment Plant (Bulaq Dakrur, Giza Governorate). This sample was used to fill the MFCs and to start the experiments. The properties of the wastewater sample were documented as follows: The values of total solids (TS), volatile solids (VS), ash, pH and organic carbon (OC) of wastewater, sludge and their mixture are listed in Table 1.

Conducting the measurements

A national instrument (NI 9207 Spring, 16-channel) was used for voltage and current measurements of all MFCs at the same time, which is important for the constant conditions of the measurements. It features eight current and eight voltage inputs, 500 samples s^{-1}, ±20 mA current inputs, ±10 V voltage inputs, 24-bit high-resolution mode, and built-in 50/60 Hz noise rejection. A portable smart water quality meter was used for measurements of pH, conductivity, total dissolved solids, salinity, temperature, and dissolved oxygen (DO). A true-RMS data logging multimeter was used for volt and current recording.

RESULTS

Microscopic characterization of nanomaterials

Figure 2(A) shows an SEM image of the CNTs, revealing their tubular structure. The synthesized CNTs had a diameter of 40–50 nm and lengths of about 20 µm. Pristine g-C_3N_4 nanosheets were observed as layered and stacked structures in the SEM image (Fig. 2(B)). They were composed of nanosheet-like structures and appeared fluffier compared to the other materials. r-GO exhibits an irregular and folded layer structure with entangled nanosheets. Figure 2(C) shows an SEM image of the r-GO, highlighting its single- or few-layer nanosheets with wrinkles. Figure 2(D) shows the XRD pattern of CNTs, including characteristic diffraction peaks at 26.52°, 42.48°, 54.71° and 78.43° 2θ, due to (220), (100), (004), and (110) reflection of planes, respectively.[29,30] The XRD pattern of refined g-C_3N_4 showed that peaks at 26.73° and 13.37° were assigned to the (002) interlayer structural packing crystal plane and (100) interplanar stacking diffraction planes, respectively. The high peak at 26.73° verifies the stacking

Table 1. Total solids (TS), volatile solids (VS), ash, pH and organic carbon of wastewater, sludge and mixture

Item	Wastewater	Sludge	Mixture
TS %	0.49 ± 0.13	3.8 ± 0.64	1.59 ± 0.15
VS %	0.44 ± 0.11	2.44 ± 0.49	1.05 ± 0.03
VS (% as TS)	90.37 ± 2.21	64.01 ± 2.12	65.97 ± 7.9
Ash	0.05 ± 0.02	1.36 ± 0.15	0.55 ± 0.18
Organic carbon (%)	52.35 ± 0.42	37.13 ± 1.23	38.26 ± 4.6
pH	6.30	6.50	6.10

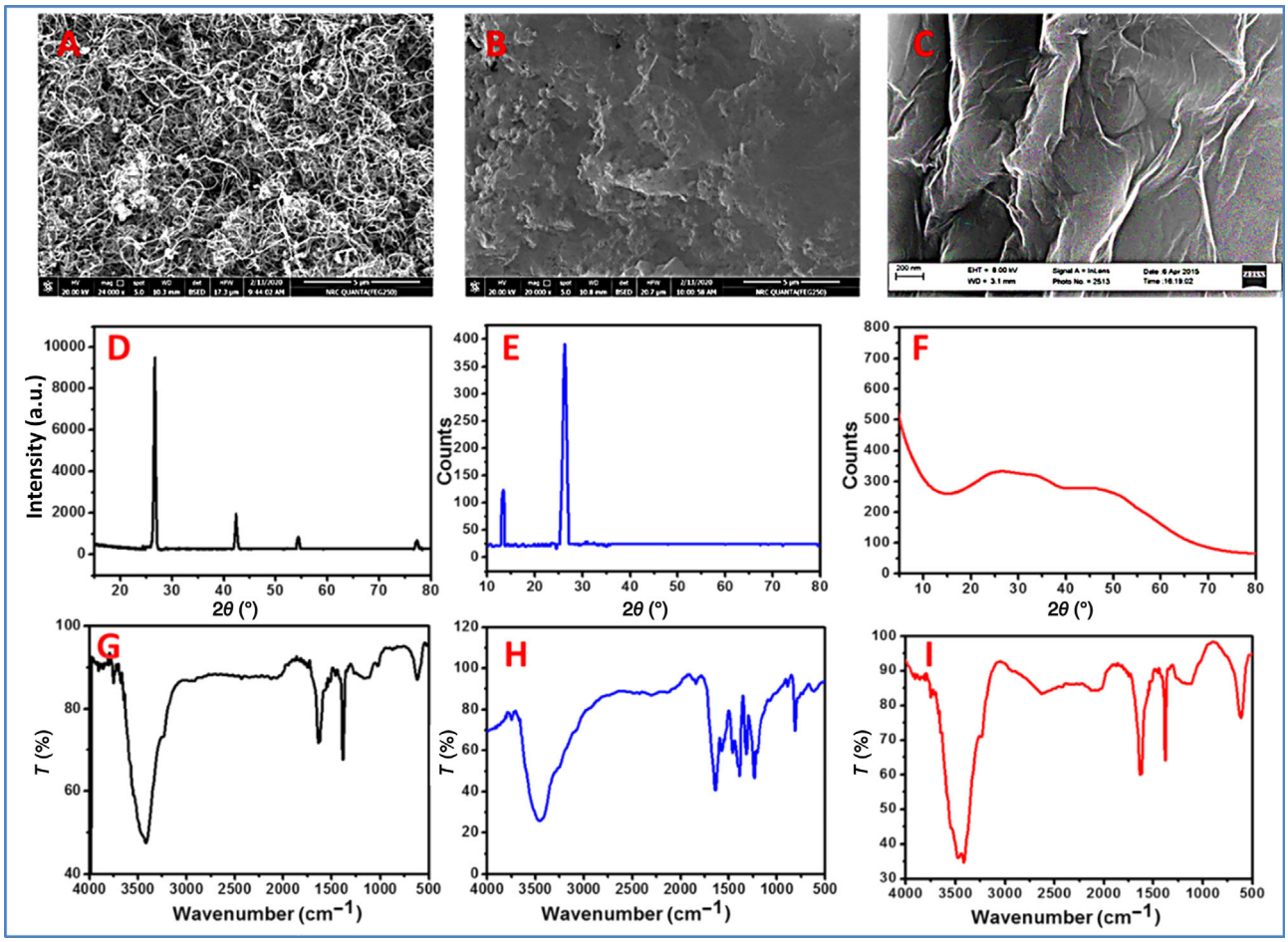

Figure 2. SEM images of the synthesized carbon nanotubes (A), g-C_3N_4 (B) and r-GO (C), respectively. XRD patterns of the prepared carbon nanotubes (D), g-C_3N_4 (E) and r-GO (F), respectively. FTIR spectra of the prepared carbon nanotubes (G), g-C_3N_4 (H) and r-GO (I), respectively.

reflection of conjugated aromatic systems, showing a graphitic structure with an interlayer distance of 0.326 nm, as shown in Fig. 2(E).[31,32] The 3D character of graphene oxide is reduced, as indicated by the disappearance of the narrow XRD reflection at $2\theta = 10.8$ A°. Instead, broadband is observed in the case of r-GO, probably due to intralayer spacing, as shown in Fig. 2(F).[33] The FTIR spectrum of raw CNTs (Fig. 2(G)) presents wide-range absorption peaks of 3450–3460 cm^{-1} resembling the —OH group, indicating the presence of hydroxyl groups on the surface of the CNTs. It was found that these groups can be subjected to oxidation of the carbon surface following exposure to air and the lack of catalysts during the synthesis. Both peaks at 2950 and 2850 cm^{-1} resemble C—H stretch vibration. The C—C trait peak is found at 1580 cm^{-1}. An additional peak at 1650 cm^{-1} is the C—O stretching mode of the functional groups on the surface of the multi- walled CNTs or evolving from the absorption of CO_2 on the composites' surface. The peak observed at 950 cm^{-1} is assigned to the C—O stretching mode. In the FTIR spectrum of g-C_3N_4, the peaks at 1145, 1213, 1393, 1587 and 1648 cm^{-1} are ascribed to the stretching modes of CN heterocycles coupled with skeletal stretching vibrations of aromatic rings, while the peak at 810 cm^{-1} matches the breathing mode of the g-C_3N_4 triazine units (Fig. 2(H)). For graphene, the bands at 1724, 1222, and 1050 cm^{-1} are ascribed to carbonyl, epoxy and alkoxide functional groups, respectively, and are considerably decreased in contrast to those of GO, implying deoxygenation of the

sheets[31-33] as shown in Fig. 2(I). The specific surface area (SSA) of the prepared r-GO was 170.98 $m^2\ g^{-1}$, while the SSAs were 209 and 89 $m^2\ g^{-1}$ for CNTs and g-C_3N_4 nanosheets, respectively.

Effects of nanomaterial addition to the electrolyte on MFCs

The results of the experiments show that the addition of trace amounts (50 mg) of CNTs, g-C_3N_4 and r-GO to the electrolyte (1.5 L) of the MFCs increases the generated electrical power by 5.21, 5.09 and 5.04 times, respectively, compared to the control with air pump. While both r-GO and CNTs increased electrical power compared to the control without air pump (5.02 and 5 times increase, respectively), incorporating g-C_3N_4 resulted in a much more significant enhancement, boosting power by a staggering 5.08 times (Fig. 3(A,B)). It was discovered that raising the oxygen supply to the cathode chamber had a beneficial impact on cell performance by increasing the voltage value. In general, cathodic chamber aeration improved microbial fuel cell efficiency over no aeration. As a result, the performance of the microbial fuel cell improved. It may be concluded that oxygen concentration influences both reaction kinetics and final power efficiency.[34,35] In our previous work, the electrogenic bacterial growth in MFCs over time before and after electricity generation was examined and the results showed that under the two MFC conditions there was an exponential increase in electrogenic bacterial growth after 20 h of operation. However, there was a slight decrease in bacterial growth after 40 h of operation as the nutrient in the MFCs started to decrease. Interestingly, higher bacterial growth was recorded in the MFCs when 50 mg CNTs was added, in comparison to control.[34]

Another issue, using a pump to introduce air (oxygen) into the cathode chamber, has a strong effect on the amount of generated power from the MFCs. In the case of using a pump and adding nanomaterials to the electrolyte, the maximum bioelectric power was generated in the cathode chamber immediately after the MFCs were operated. The voltage value averaged 1301 mV, with an average areal power density of 21.05 mW m^{-2} and an average volumetric power density of 14.11 mW m^{-3} when adding CNTs to the electrolyte with a constant loading resistance of 80 kΩ and it showed voltage stability until the end of the 140 h interval. However, in the control experiment (without nanomaterial addition), which is the conventional method, the voltage value of the control reached its maximum value after 15 h and averaged 570 mV, with an average areal power density of 4.04 mW m^{-2} and an average volumetric power density of 2.7 mW m^{-3}; with constant loading resistance of 80 kΩ it then showed voltage stability until the end of the 140 h interval. Thereby, the electrical conductivity of MFCs was improved, leading to an increase in

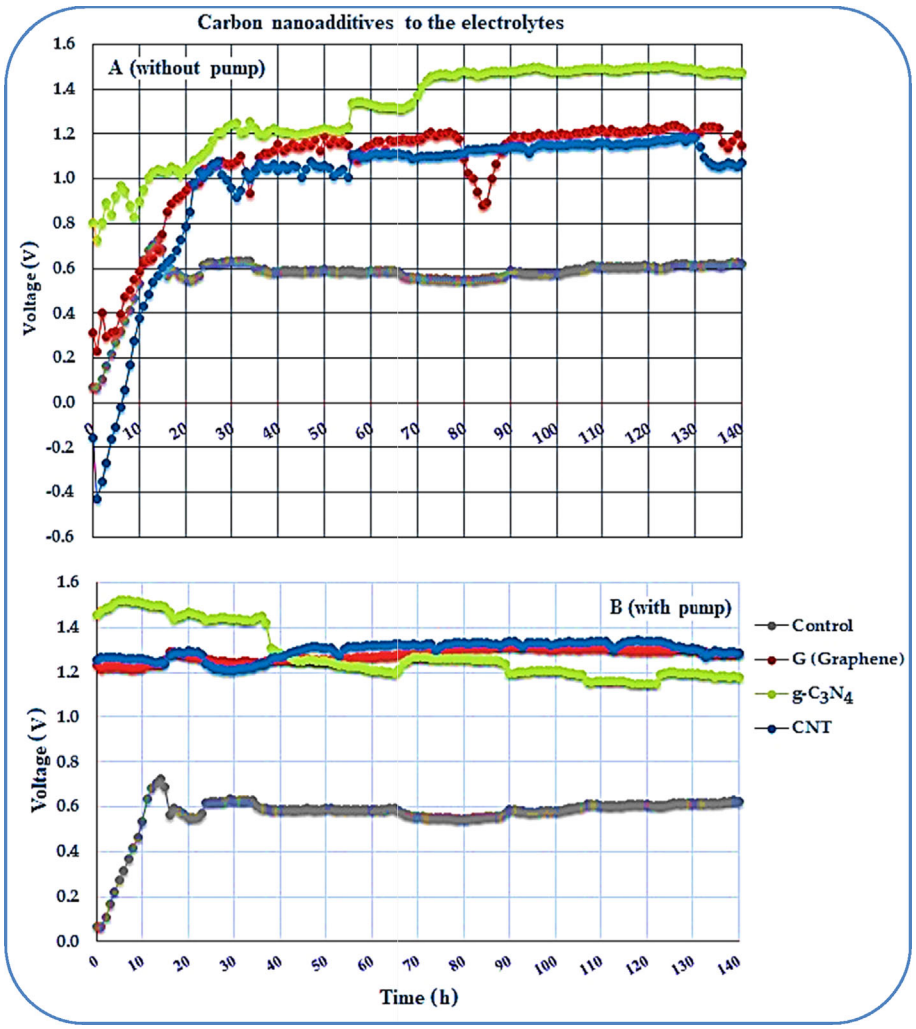

Figure 3. Voltage of the MFCs (A) without pump and (B) with pump, which was used to introduce air into the cathode chamber.

Table 2. Highest voltage (V), electric current (I), resistance (R), power (P), aerial power density (P_{AD}), projected surface area of the anode (A), Volume (V), and volumetric power density (P_D) of all treatments.

Nanoadditives	*V* (V)	*I* (A)	*R* (kΩ)	*P* (W)	*v* (m^3)	P_D (mW m^{-3})	*A* (m^2)	P_{AD} (mW m^{-2})
CNTs	1.301	1.626E−05	80	2.11575E−05	1.50E−03	14.11	1.00E−03	21.06
g-C_3N_4	1.286	1.607E−05	80	2.06721E−05	1.50E−03	13.78	1.00E−03	20.57
r-GO	1.280	1.600E−05	80	2.04878E−05	1.50E−03	13.66	1.00E−03	20.39
Control	0.570	0.713E−05	80	0.40612E−05	1.50E−03	2.71	1.00E−03	4.04

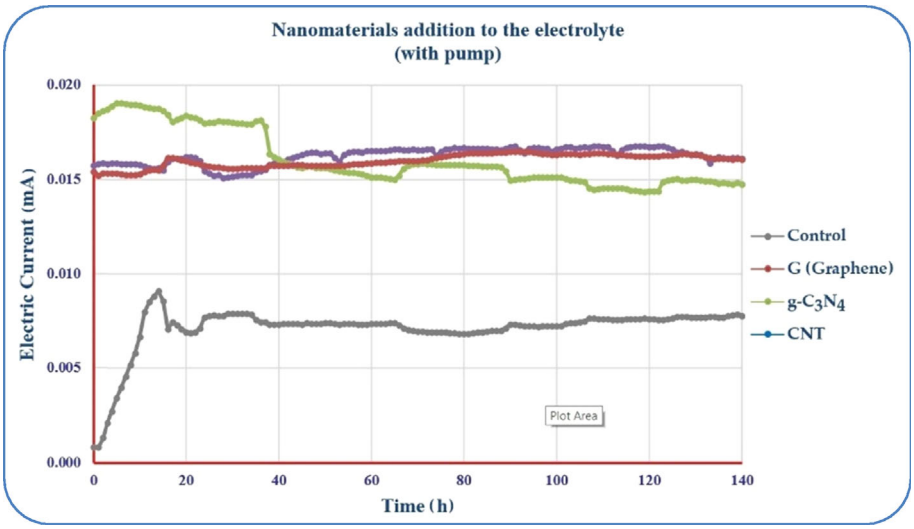

Figure 4. Electric current of the MFCs, where a pump was used to introduce air into the cathode chamber.

the generated power by 5.21 times the control. Table 2 shows these data for all treatments.

The electric current of the MFCs where a pump was used to introduce air into the cathode chamber was plotted for all treatments (Fig. 4). For each curve, the total coulombs were computed as the integration of electric current to time and then divided by the theoretical coulombs to estimate the coulombic efficiency of the MFC. The results show the coulombic efficiency of the MFC, where additions of CNTs, g-C_3N_4 and r-GO to the electrolyte of MFC compared to the control were 19.43%, 19.19%, 19.11%, and 8.54%, respectively.

The stability of the examined r-GO, g-C_3N_4, and CNT nanoadditives was studied by following the current of the constructed MCF over time for up to 140 h. The obtained results were compared with that of the control cell in (Fig. 5). Graphene and CNTs displayed stable current values within the whole measurement time to reveal their improved stability performance when applied to the MCF structure. On the other hand, the current of g-C_3N_4 gradually decayed within the initial few hours until 40 h; afterward, its current was steadily stabilized. The control cell exhibited a sharp current increase when starting the measurement up until 14 h had passed. A steady current was then shown. This steady current at 120 h using the three carbon nanoadditives compared with that in the control cell was, in ascending order, control cell [7.606 μA] > g-C_3N_4 [14.384 μA] > r-GO [16.230 μA] > CNTs [16.768 μA]. Generally, the current (stability) decay after fuel cell operation for an extended time could be attributed to the accumulation of the reaction byproducts on the investigated carbon surfaces, leading to poisoning of the active sites for further reactant adsorption. Corrosion of the carbon support material and its leaching in the tested medium also played a role in reducing the available surface area for the studied reaction.[36] The obtained results in this stability experiment for g-C_3N_4, r-GO and CNTs confirmed those shown by the whole study, encouraging their application in MFC structures, especially r-GO and CNTs. Histograms of these carbon types for the measured stability currents at varied time intervals (Fig. 6) demonstrated that their performance was highly stable within the whole stability experiment period.

DISCUSSION

The present study concentrated on applying MFCs to the production electrical power from wastewater. This wastewater is produced in huge amounts annually and then exposed to physical, biological and chemical remediation methods in wastewater treatment plants. Thus, this method would not only treat wastewater but also produce electricity. Nevertheless, MFC implementation in wastewater treatment plants is limited due to electrolyte resistance, which is one of the major factors limiting electricity generation. This research focused on using nanomaterials as an additive to the electrolyte of MFCs for improving electrical power generation from wastewater. Consequently, the productivity of the MFC rose.

Extracellular electron transfer (EET) is a process that involves moving electrons from the anode to the microorganisms.[37] EET often takes place in MFC through direct and indirect electron transfer pathways: (i) electrically conducting pili, (ii) extracellular substances and (iii) conductive materials are the three primary methods that have been studied so far regarding direct electron transfer in biological systems.[38,39] Short direct electron transfer

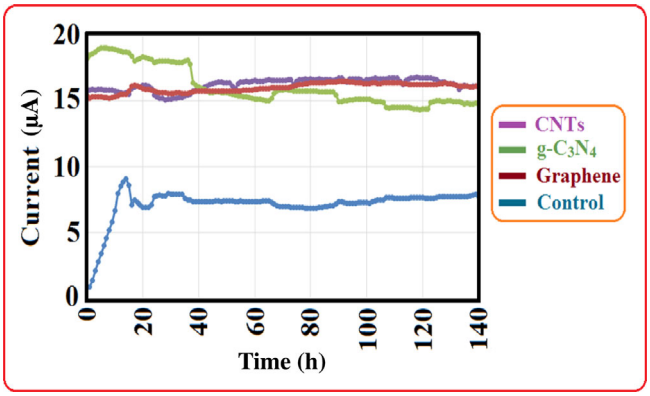

Figure 5. Variation of current values with elapsed time at r-GO, g-C_3N_4 and CNTs in comparison with that in the control cell.

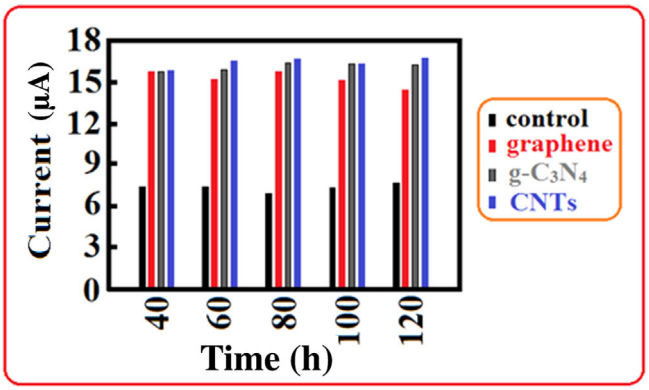

Figure 6. Histograms of current values of r-GO, g-C_3N_4 and CNTs in comparison with that in the control cell at certain time intervals within the whole stability experiment.

requires the presence of biofilm in close physical contact with the anode. Nanomaterials can modify the anode compartment by increasing its conductivity and surface area, increasing electron transfer through the mediator and through the biofilm, as well as enhancing biocompatibility and colonization, which promotes a favorable environment for the growth of microorganisms on the electrode surface and improves MFC performance. Nanomaterials can provide a high specific surface area for the adhesion and growth of the microorganisms around the anode, thereby facilitating the direct electron transfer (DIET) process. Conductive carbon nanomaterials play the role of a bridge between the microorganisms and the anode to promote the DIET in MFCs. Conductive materials can also result in closely connected microbial communities.[40,41] In most cases, the interface between the anode and the exoelectrogens is embellished with carbon-based nanomaterials. They not only retain the overall benefits of traditional carbon materials but also demonstrate a high surface area that is advantageous for bacterial adhesion and increases the number of EET contacting active areas.[42] The huge specific surface area of CNTs creates ideal conditions for the adhesion and proliferation of electroactive bacteria, and the local concentrations of exoelectrogens are advantageous to the rate of electron transfer from bacteria to anode. CNTs are said to have cytotoxicity compared to g-C_3N_4, which can stop cell growth and even result in cell death.[43] As a result, the CNT dose needs to be carefully monitored.

Using high resistance in MFCs has been shown to improve the specific energy output through several underlying mechanisms. First, high resistance limits the flow of current, creating a controlled environment for electron transfer. This enhances electron transfer efficiency from the anode chamber to the cathode chamber, resulting in improved energy conversion efficiency and specific energy output. Second, high resistance conditions favor the growth and activity of exoelectrogenic bacteria responsible for electron transfer. These bacteria adapt to high resistance by developing more efficient electron transfer pathways, leading to enhanced energy output per unit of substrate consumed. Additionally, high resistance can reduce energy losses due to internal resistance within the MFC, resulting in a higher proportion of available energy being converted into electrical output.

In accordance with the existing investigation, preceding studies have shown the utilization of different materials in the electrolyte of MFCs. Antolini[44] has investigated composite materials for polymer electrolyte membrane MFCs. Precisely, Ahmed *et al.*[45] stated that a maximum power density was attained using the CoOx–CoPc/C cathode as it was 37% higher than that of FePc/C. Besides, Wu *et al.*[14] implemented low substrate COD concentrations to enhance the performance of MFCs. In the current study, however, nanomaterials were used as substrate (electrolyte) additives instead of lowering the COD concentration. Therefore, it can be assumed that the innovation trend of adding materials to the electrolyte is in line with the current investigation, but with different results due to the application of different types of materials – nanomaterials –which ultimately delivered different output voltages. Further studies have investigated different materials other than nanomaterials, such as oxygen-saturated electrolytes[46] and montmorillonite.[47] Considering that in the anode chamber an anaerobic digestion process takes place, previous studies have investigated the effects of using nanomaterials and trace metals in the anaerobic digestion process.[48,49] Besides, life cycle assessment research investigated the utilization of nanomaterials in the anaerobic digestion process of manure.[50]

Beyond improving conductivity, nanomaterials also provide a high surface area for microbial adhesion and biofilm formation. The increased surface area allows for a greater density of exoelectrogenic bacteria, which are responsible for directly converting organic matter into electricity. This leads to enhanced biocatalytic activity and higher electricity generation. Nanomaterials like CNTs and r-GO can act as bridges between microbes and the electrode, facilitating the transfer of electrons directly to the electrode surface. This process, known as direct electron transfer (DIET), bypasses the electron shuttle pathway and leads to faster electron transfer and higher energy conversion efficiency. These findings are in agreement with the study by Starowicz *et al.*, in which the use of r-GO as an electrode in MFCs and reports increased bioelectricity generation and nutrient removal, potentially due to enhanced DIET.[51] Also, Wilberforce *et al.* investigated the use of CNTs as an electrode in MFCs and observed the improved power generation and coulombic efficiency, with evidence suggesting DIET as a contributing factor.[52] Another study demonstrates that adding granular activated carbon (GAC) to methanogenic digesters enhances DIET between bacteria and methanogens, leading to increased methane production.[53]

Nanomaterials can be modified to improve their biocompatibility, promoting the growth and activity of beneficial microbes in the MFC anode. Additionally, nanomaterials can enhance the stability and structure of the microbial biofilm, leading to a more robust and efficient MFC operation. Studies have shown that

incorporating nanomaterials into MFCs can significantly enhance their performance. The addition of CNTs has been shown to increase power generation by up to five times compared to control MFCs. Similarly, other nanomaterials like g-C_3N_4 and r-GO have also demonstrated promising results in increasing power density and coulombic efficiency. This can be attributed to the fact that the addition of nanomaterials biostimulates the anaerobic digestion taking place in the anode chamber.[54] Despite the promising potential of nanotechnology in MFCs, some challenges remain. These include the cost and scalability of nanomaterial synthesis, long-term stability of nanomaterials in the MFC environment and potential environmental concerns related to nanomaterial release. Future research efforts should focus on addressing these challenges and developing novel nanomaterials that are specifically tailored for MFC applications.

CONCLUSIONS

The incorporation of carbon-based nanomaterials into the electrolytes of MFCs leads to a substantial improvement in bioelectricity generation, with a 5.21-fold increase compared to the control. Additionally, coulombic efficiency is boosted by 2.28 times when compared to the control. The field of nanotechnology provides a potent tool for enhancing the performance and scalability of MFCs. By enhancing conductivity, fostering microbial growth and accelerating direct electron transfer, nanomaterials like carbon nanotubes, graphitic carbon nitride and reduced graphene oxide pave the way for significant advancements in this promising technology. This translates to cleaner wastewater treatment, more efficient bioenergy generation and a step closer to sustainable solutions for our future. Through various mechanisms such as enhanced conductivity, stimulation of microbial growth and facilitation of direct electron transfer, nanomaterials like carbon nanotubes, graphitic carbon nitride and reduced graphene oxide can significantly contribute to the advancement of this promising technology. This progress holds great potential for sustainable wastewater treatment and the generation of bioenergy.

AUTHOR CONTRIBUTIONS

EMA participated in the experimental design and setup, resources, writing – review and editing. MS participated in conceptualization, resources, experimental design and setup, writing original draft, review, editing, and project administration as co-principal investigator. MSM participated in the isolation, cultivation and growth of bacteria. MS, EM, HE and RMA participated in the experimental design and setup. MS provided different samples of wastewater for MFCs. YAA participated in the experimental design, writing – review and editing, and project administration as principal investigator, and funding acquisition. All the authors read and approved the revised manuscript.

ACKNOWLEDGEMENTS

The authors acknowledge the financial support of Cairo University in the framework of Project No. 143-2017.

DATA AVAILABILITY STATEMENT

All data generated or analyzed during this study are included in this published article.

REFERENCES

1 Papaharalabos G, Greenman J, Melhuish C and Ieropoulos I, A novel small-scale microbial fuel cell design for increased electricity generation and wastewater treatment. *Int J Hydrogen Energy* **40**:4263–4268 (2015).
2 Alzate-Gaviria L, Microbial fuel cells for wastewater treatment, in *Wastewater – Treatment and Reutilization*, ed. by Einschlag F. InTech Europe, Rijeka (2011). https://doi.org/10.5772/15546.ISBN: 978-953-307-249-4
3 Karmakar S, Kundu K and Kundu S, Design and development of microbial fuel cells in Current Research, Technology and Education Topics in Applied Microbiology and Microbial Biotechnology (ed. A. Mendez-Vilas) 1029–1034 (Formatex Research Center) (2010).
4 Vidhyeswari D, Surendhar A and Bhuvaneshwari S, General aspects and novel PEMss in microbial fuel cell technology: a review. *Chemosphere* **309**:136454 (2022).
5 Kugarajah V, Sugumar M and Dharmalingam S, Nanocomposite membrane and microbial community analysis for improved performance in microbial fuel cell. *Enzyme Microb Technol* **140**:109606 (2020).
6 Aelterman P, Rabaey K, Pham HT, Boon N and Verstraete W, Continuous electricity generation at high voltages and currents using stacked microbial fuel cells. *Environ Sci Technol* **40**:3388–3394 (2006).
7 Zhao Y, Watanabe K, Nakamura R, Mori S, Liu H and Hashimoto IK, Three-dimensional conductive nanowire networks for maximizing anode performance in microbial fuel cells. *Chem – Eur J* **16**:4982–4985 (2010).
8 Yang W and Chen S, Biomass-derived carbon for electrode fabrication in microbial fuel cells: a review. *Ind Eng Chem Res* **59**:6391–6404 (2020).
9 Carrillo-Peña D, Mateos R, Morán A and Escapa A, Reduced graphene oxide improves the performance of a methanogenic biocathode. *Fuel* **321**:23957 (2022).
10 Luo J, Li M, Zhou M and Hu Y, Characterization of a novel strain phylogenetically related to *Kocuriarhizophila* and its chemical modification to improve performance of microbial fuel cells. *Biosens Bioelectron* **69**:113–120 (2015).
11 An J, Sim J and Lee H-S, Control of voltage reversal in serially stacked microbial fuel cells through manipulating current: significance of critical current density. *J Power Sources* **283**:19–23 (2015).
12 Madani S, Gheshlaghi R, Mahdavi MA, Sobhani M and Elkamel A, Optimization of the performance of a double-chamber microbial fuel cell through factorial design of experiments and response surface methodology. *Fuel* **150**:434–440 (2015).
13 Prasath SS and Arockiarajan A, Effect of interphase and thermal environment on the effective properties of macro-fiber composites (MFC). *Compos Part B* **75**:327–335 (2015).
14 Wu S, Liang P, Zhang C, Li H, Zuo K and Huang X, Enhanced performance of microbial fuel cell at low substrate concentrations by adsorptive anode. *Electrochim Acta* **161**:245–251 (2015).
15 Zhang C, Liang P, Jiang Y and Huang X, Enhanced power generation of microbial fuel cell using manganese dioxide-coated anode in flow-through mode. *J Power Sources* **273**:580–583 (2015).
16 Baranitharan E, Khan MR, Prasad D, Teo W, Tan G and Jose R, Effect of biofilm formation on the performance of microbial fuel cell for the treatment of palm oil mill effluent. *Bioprocess Biosyst Eng* **38**:15–24 (2015).
17 Vilajeliu-Pons A, Puig S, Pous N, Salcedo-Dávila I, Bañeras L, Balaguer MD *et al.*, Microbiome characterization of MFCs used for the treatment of swine manure. *J Hazardous Mater* **288**:60–68 (2015).
18 Joshi SS, Patil PR, Naimase MS and Bakare PP, Role of ligands in the formation, phase stabilization, structural and magnetic properties of Fe_2O_3 nanoparticles. *J Nanopart Res* **5**:635–643 (2006).
19 Petcharoen K and Sirivat A, Synthesis and characterization of magnetite nanoparticles via the chemical co-precipitation method. *J Mater Sci Eng B* **177**:421–427 (2012).
20 Kumar SS, Venkateswarlu P, Rao VR and Rao GN, Synthesis, characterization and optical properties of zinc oxide nanoparticles. *Int Nano Lett* **3**:30 (2013).
21 Kumar H, Manisha and Sangwan P, Synthesis and characterization of MnO_2 nanoparticles using Co-precipitation technique. *Int J Chem Chem Eng* **3**:155–160 (2013).
22 Janicek A, Fan Y and Liu H, Performance and stability of different cathode base materials for use in microbial fuel cells. *J Power Sources* **280**:159–165 (2015).

23 Rabaey K and Verstraete W, Microbial fuel cells: novel biotechnology for energy generation. *Trends Biotechnol* **23**:291–298 (2005).
24 Attia YA, Mohamed YMA and Altalhi TA, Photobiosynthesis of metal/graphene nanocomposites: new materials for water desalination and purification. *Desalin Water Treat* **57**:26014–26021 (2016).
25 Attia YA, Vázquez-Vázquez C and Mohamed YMA, Facile production of vitamin B_3 and other heterocyclic carboxylic acids using an efficient Ag/ZnO/graphene-Si hybrid Nanocatalyst. *Res Chem Intermed* **43**: 203–218 (2017).
26 Attia YA, Attia SY, Essa R and Mohamed S, Photosynthesis of chromium oxide/reduced graphene oxide nanocomposites and its application in water desalination and purification. *Nanosci Nanotechnol -Asia* **10**: 719–725 (2020).
27 Altalhi T, Mezni A, Aldalbahi A, Alrooqi A, Attia YA, Santos A *et al.*, Fabrication and characterisation of sulfur and phosphorus (S/P) co-doped carbon nanotubes. *Chem Phys Lett* **658**:92–96 (2016).
28 Attia YA, Al Nazawi AM, Elsayed H and Sadik MW, Carbon nanotubes catalyzed UV-trigger production of hyaluronic acid from *Streptococcus equi*. *Saudi J Biol Sci* **28**:484–491 (2021).
29 Attia YA and Mohamed YMA, Silicon-grafted Ag/AgX/rGO nanomaterials (X= Cl or Br) as dip-photocatalysts for highly efficient p-nitrophenol reduction and paracetamol production. *Appl Organomet Chem* **33**:4757 (2019).
30 Attia YA, Ag/ZnO/graphene-TBSCl hybrid nanocomposite as highly efficient catalyst for hydrogen production. *Mater Express* **6**:211–219 (2016).
31 Verma S and Varma RS, Photocatalytic oxidation of aromatic amines using MnO_2@g-C_3N_4. *Adv Mater Lett* **8**:754–756 (2017).
32 Yue X, Yi S, Wang R, Zhang Z and Qiu S, Cadmium sulfide and nickel synergetic co-catalysts supported on graphitic carbon nitride for visible-light-driven photocatalytic hydrogen evolution. *Sci Rep* **6**: 22268 (2016).
33 McAllister MJ, Li J-L, Adamson DH, Schniepp HC, Abdala AA, Liu J *et al.*, Single sheet functionalized graphene by oxidation and thermal expansion of graphite. *Chem Mater* **19**:4396–4404 (2007).
34 Attia YA, Samer M, Mohamed MSM, Moustafa E, Salah M and Abdelsalam EM, Nanocoating of microbial fuel cell electrodes for enhancing bioelectricity generation from wastewater. *Biomass Convers Biorefin* **14**:847–858 (2022). https://doi.org/10.1007/s13399-022-02321-7.
35 Moustafa E, Abdelsalam E, Attia Y, Mohamed MSM, Salah M, Moselhy MA *et al.*, Enhancing the performance of microbial fuel cells by installing an air pump to the cathode chamber. *Egypt J Chem* **64**: 5471–5476 (2021).
36 Zhou WJ, Song SQ, Li WZ, Zhou ZH, Sun GQ, Xin Q *et al.*, Direct ethanol fuel cells based on PtSn anodes: the effect of Sn content on the fuel cell performance. *J Power Sources* **140**:50–58 (2005).
37 Kumar A, Huan-Hsuan Hsu L, Kavanagh P, Barrière F, Lens PNL, Lapinsonniere L *et al.*, The ins and outs of microorganism–electrode electron transfer reactions. *Nat Rev Chem* **1**:0024 (2017). https://doi.org/10.1038/s41570-017-0024.
38 Lovley DR, Syntrophy goes electric: direct interspecies electron transfer. *Annu Rev Microbiol* **71**:643–664 (2017).
39 Lovley DR, Electrically conductive pili: biological function and potential applications in electronics. *Curr Opin Electrochem* **4**:190–198 (2017).
40 Narayanasamy S and Jayaprakash J, Chapter 6 – nanostructures and nanomaterials in microbial fuel cells, in *Micro and Nano Technologies, Nanotechnology in Fuel Cells*, ed. by Song H, Nguyen TA and Yasin G. Elsevier, Amsterdam, pp. 139–171 (2022) ISBN 9780323857277.
41 Mohamed HO, Sayed ET, Obaid M, Choi Y-J, Park S-G, Al-Qaradawi S *et al.*, Transition metal nanoparticles doped carbon paper as a cost-effective anode in a microbial fuel cell powered by pure and mixed biocatalyst cultures. *Int J Hydrogen Energy* **43**:21560–21571 (2018).
42 Hindatu Y, Annuar M, Subramaniam R and Gumel A, Medium-chain-length poly-3-hydroxyalkanoates-carbon nanotubes composite anode enhances the performance of microbial fuel cell. *Bioprocess Biosyst Eng* **40**:919–928 (2017).
43 Cai T, Huang M, Huang Y and Zheng W, Enhanced performance of microbial fuel cells by electrospinning carbon nanofibers hybrid carbon nanotubes composite anode. *Int J Hydrogen Energy* **44**:3088–3098 (2019).
44 Antolini E, Composite materials for polymer electrolyte membrane microbial fuel cells. *Biosens Bioelectron* **69**:54–70 (2015).
45 Ahmed J, Yuan Y, Zhou L and Sunghyun KS, Carbon supported cobalt oxide nanoparticles–iron phthalocyanine as alternative cathode catalyst for oxygen reduction in microbial fuel cells. *J Power Sources* **208**:170–175 (2012).
46 Khomenko VG, Barsukov VZ and Katashinskii AS, The catalytic activity of conducting polymers toward oxygen reduction. *Electrochim Acta* **50**:1675–1683 (2005).
47 Hasani-Sadrabadi MM, Dashtimoghadam E, Eslami SNS, Bahlakeh G, Shokrgozar MA and Jacob KI, Air-breathing microbial fuel cell with enhanced performance using nanocomposite proton exchange membranes. *Polymer* **55**:6102–6109 (2014).
48 Abdelsalam E, Samer M, Attia Y, Abdel-Hadi MA, Hassan HE and Badr Y, Effects of laser irradiation and Ni nanoparticles on biogas production from anaerobic digestion of slurry. *Waste Biomass Valori* **10**: 3251–3262 (2019).
49 Hijazi O, Abdelsalam E, Samer M, Amer BMA, Yacoub IH, Moselhy MA *et al.*, Environmental impacts concerning the addition of trace metals in the process of biogas production from anaerobic digestion of slurry. *J Clean Prod* **243**:118593 (2020).
50 Hijazi O, Abdelsalam E, Samer M, Attia YA, Amer BMA, Amer MA *et al.*, Life cycle assessment of the use of nanomaterials in biogas production from anaerobic digestion of manure. *Renew Energy* **148**:417–424 (2020).
51 Starowicz A, Zieliński M, Rusanowska P and Dębowski M, Microbial fuel cell performance boost through the use of graphene and its modifications—review. *Energies* **16**:576 (2023).
52 Wilberforce T, Abdelkareem MA, Elsaid K, Olabi AG and Sayed ET, Role of carbon-based nanomaterials in improving the performance of microbial fuel cells. *Energy* **240**:122478 (2022).
53 Xiao L, Lichtfouse E and Kumar PS, Advantage of conductive materials on interspecies electron transfer-independent acetoclastic methanogenesis: a critical review. *Fuel* **305**:121577 (2021).
54 Abdelsalam E, El-Hussein A and Samer M, Photobiostimulation of anaerobic digestion by laser irradiation and photocatalytic effects of trace metals and nanomaterials on biogas production. *Int J Energy Res* **45**:141–150 (2021).

